A STUDY OF DECREASE BURST STRENGTH ON COMPRESSED-HYDROGEN CONTAINERS BY DROP TEST

Masuda, S.[1], Tomioka, J.[2] , Tamura, H.[3] and Tamura, Y.[4]
[1] E-mobility Research Division, Japan Automobile Research Institute, 1328-23, Osaka, Shirosato, Ibaraki, 311-4316, Japan, mshun@jari.or.jp
[2] E-mobility Research Division, Japan Automobile Research Institute, 1328-23, Osaka, Shirosato, Ibaraki, 311-4316, Japan, jtomioka@jari.or.jp
[3] E-mobility Research Division, Japan Automobile Research Institute, 1-1-30, Shibadaimon, Minato-ku, Tokyo, 105-0012, Japan, thiroaki@jari.or.jp
[4] E-mobility Research Division, Japan Automobile Research Institute, 1328-23, Osaka, Shirosato, Ibaraki, 311-4316, Japan, ytamura@jari.or.jp

ABSTRACT

We investigate an appropriate initial burst pressure of compressed hydrogen containers that correlates with a residual burst pressure requirement at the end of life (EOL) and report an influence of hydraulic sequential tests on residual burst pressure. Results indicate that a container damage caused by a drop test during hydraulic sequential tests has a large influence on burst pressure. The container damage induced through hydraulic sequential tests is investigated using nondestructive evaluations to clarify a strength decreasing mechanism. An ultrasonic flaw detection analysis is conducted before and after the drop test and indicated that the damage occurred at the cylindrical and dome parts of the container after the drop test. An X-ray computed tomography imaging identifies a delamination inside laminated structure made of carbon fiber reinforced plastics (CFRP) layer, with some degree of delamination reaching the end boss of the container. Results suggest that a load profile fluctuates in the CFRP layer at the dome part and that a burst strength of the dome part decreases. Therefore, an observed decreasing in drop damage at the dome part can be used to prevent a degradation of EOL container burst strength.

NOMENCLATURE

CFRP : Carbon fiber reinforced plastics
CT : Computed tomography
EC79 : European Communities Regulation No 79
EOL : End of life
GTR13 : Global Technical Regulation No.13 (Hydrogen and fuel cell vehicles)
NWP : Nominal working pressure

1.0 INTRODUCTION

The Global technical regulation No. 13 (GTR13) Phase 1 [1], which is the global technical regulation on hydrogen and fuel cell vehicles, was adopted in June 2013. The revised version (Phase 2) is currently being deliberated. One of the key concepts of these regulations is an assurance of sufficient strength of compressed hydrogen container throughout its service life by requiring the container to retain a minimum residual burst strength of at least 180% of its nominal working pressure (NWP) at the end of life (EOL). New hydraulic sequential testing on a durability of containers was introduced in accordance with this concept to verify the residual burst strength of containers at the EOL. However, an initial burst pressure at the beginning of life is defined to be 225% NWP in current GTR13, and this value has been validated using conventional requirements. An appropriate minimum burst pressure criterion is required to reduce the cost and weight of the container. Therefore, the initial burst pressure that is correlated with EOL burst strength is required. This theme is one of the discussion tasks for Phase 2. A appropriate burst pressure that correlates with the residual burst pressure has been discussed. Recent investigations have demonstrated an influence of residual burst pressure on hydraulic sequential testing [2]. The residual burst strength of container after hydraulic sequential testing is 5% lower than the burst strength of new container; therefore, an impact site during vertical drop test may become the initial rupture point. It is also found that the bursting pressure variation becomes large. In the current study, the container damages caused by hydraulic sequential tests are analyzed in detail by performing various nondestructive

evaluations and the mechanism of container deterioration is clarified.

2.0 TEST METHOD

2.1 Overview of Test Items

Figure 1 shows a schematic diagram of the hydraulic sequential tests. One of the requirement for sequential testing is a drop test that simulates an accidental container drop during manufacturing. It includes vertical, horizontal, and oblique [45°] directions as shown in Figure 2. A nondestructive evaluation is performed on containers before and after the drop test to investigate the degree of deterioration. An ultrasonic flaw detection test, which is a simple nondestructive evaluation method, is conducted on an entire container before and after the drop test (Section 3.1). An X-ray computed tomography (CT) imaging of the damaged portion identified via the ultrasonic flaw detection test is accurately investigated to characterize its damaged state (Section 3.2). The epoxy resin in the CFRP of the containers after the drop test is gasified and removed, and an existence of damaged carbon fiber is investigated (Section 3.3). Finally, the X-ray CT imaging is conducted to investigate an influence of pressure cycling test on container damage. It is predicted that the CFRP damage generated during the drop test propagates during a later pressure cycling test (Section 3.4).

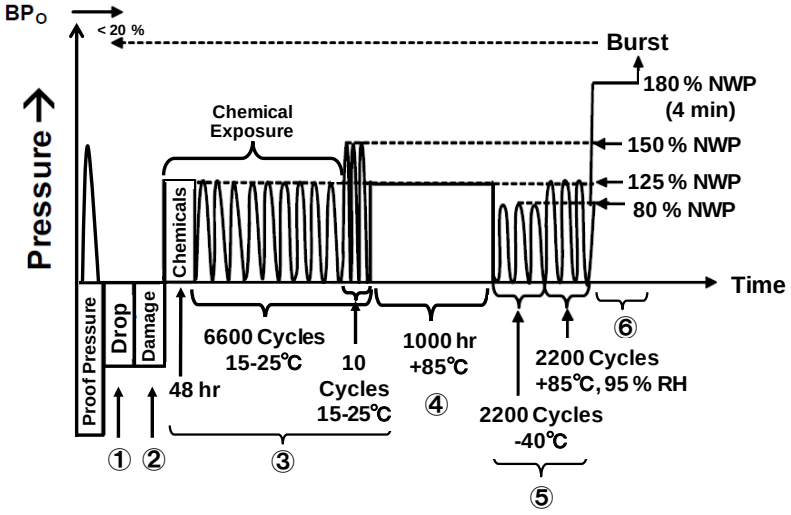

Figure 1. Hydraulic sequential tests stated in GTR13

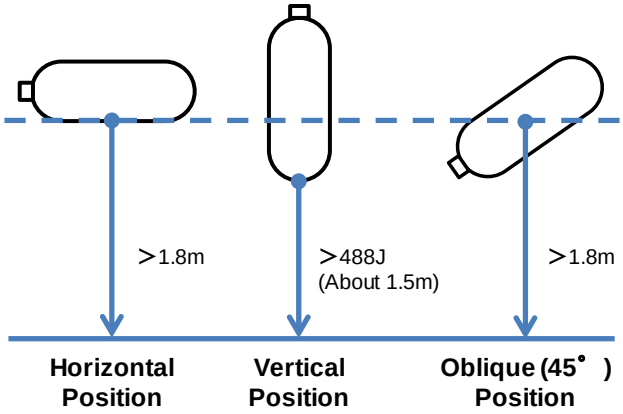

Figure 2. Positions of the drop tests in the sequential tests

2.2 Test Container Specifications

Table 1 shows the specifications of the containers used for the tests. The containers are designed according to EC79 regulation [3] and consisted of type 4 containers with entire plastic liners that are fully wrapped with CFRP resin.

2.3 Ultrasonic Flaw Detection

The flaw detection test was performed using the phased array ultrasonic inspection method [4], which can set the direction and depth of the ultrasonic beam arbitrarily. The machine oil, which is the contact medium, was applied to the measurement point, and measured the curved surface, such as the dome part of container, using a flexible probe. The pulse voltage for ultrasonic wave generation was 200 V, and the pulse width was 100 ns. The incident angle of incident wave was 0° (perpendicular to the container surface), and flaw detection was performed on the entire container. Figure 3 shows a schematic diagram of the ultrasonic flaw detection test.

Table 1. Specifications of the tested type 4 container

Reinforcing material	CFRP
Molding method	Filament winding
Nominal working pressure	70 MPa
Volume	36 L
Application criteria	EC79
Liner material	Plastic
Protector	No protector

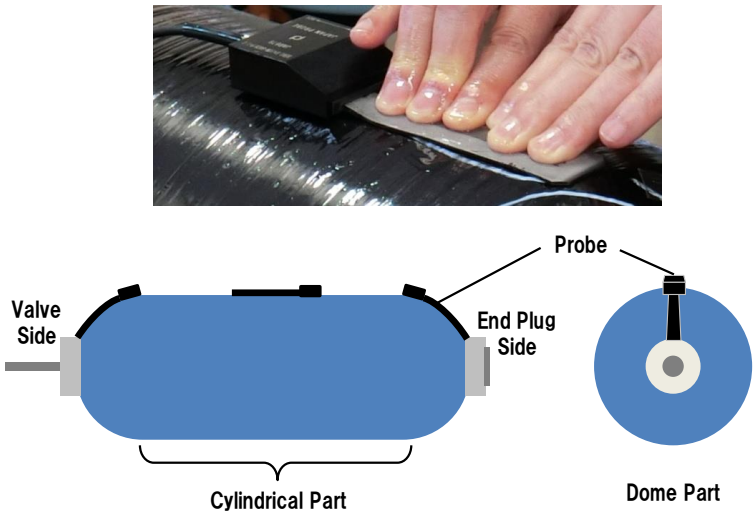

Figure 3. Schematic of the ultrasonic flaw detection system

2.4 X-ray CT Scanning

An industrial X-ray CT system [5] is used for internal inspection of the container. This system supplies high-resolution images while working at high energies. Table 2 shows the system details. The container has a round shape, and composite 3D images are created with image analysis software.

Table 2. Specifications of the high-energy X-ray CT system

Maximum X-ray energy	9 MeV
Slice thickness	0.5 mm
Image resolution	3000 pixels × 3000 pixels
Pixel size	0.2 mm × 0.2 mm

2.5 Investigation of Carbon Fiber Damage

The burn-off test was conducted to extract the carbon fiber from the CFRP. In the burn-off test, the

CFRP was heated and maintained at approximately 500 °C using an electric furnace to gasify the epoxy resin. In this way, the carbon fiber can be extracted while maintaining the original shape of the test piece. The degree of damage was investigated by analyzing the carbon fiber surface.

3.0 TEST RESULTS

3.1 Investigation of Damage via Ultrasonic Flaw Inspection

Ultrasonic testing was conducted before and after the drop test. Figure 4 shows the measurement results of the drop test at the landing area around the dome part of plug side. The blue regions indicate that sound-wave reflections were not present, and the transition to red regions indicates a layer boundary or imperfection (e.g., air layer). The range of approximately 10 mm from the outside surface is shown in red; owing to the short distance to the probe, the reflection cannot be measured well. A comparison of the containers before and after the drop test revealed a clear reflection at approximately 20–25 mm depth. This reflection coincides with the boundary between the CFRP layer and plastic liner. Furthermore, a reflection is observed at a depth of approximately 15 mm after the drop test and extends parallel to the CFRP surface. This reflection is likely due to the damage incurred during the drop test because it is not observed in the container before the drop test. Figure 5 shows the measurement results for the landing site of the cylindrical part both before and after the drop test. Damage was incurred during the drop test, similar to that observed in the dome part. Figure 6 shows a summary of the test results. No damage was incurred away from the landing site of the drop tests, whereas the CFRP layer was damaged in all three directions (vertical, horizontal, and oblique directions) near the landing site.

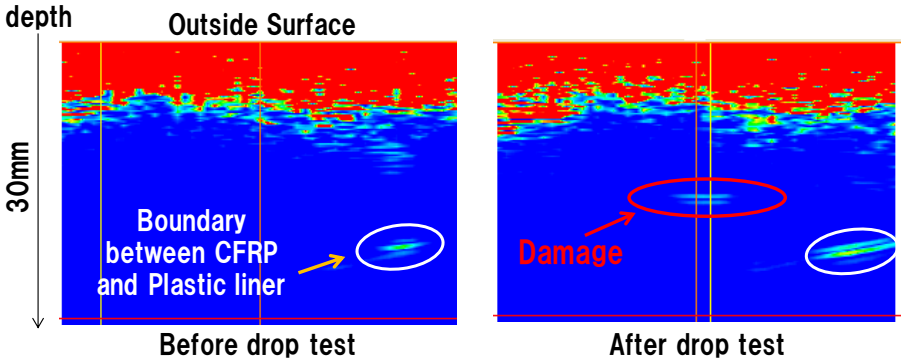

Figure 4. Ultrasonic inspection images (dome part)

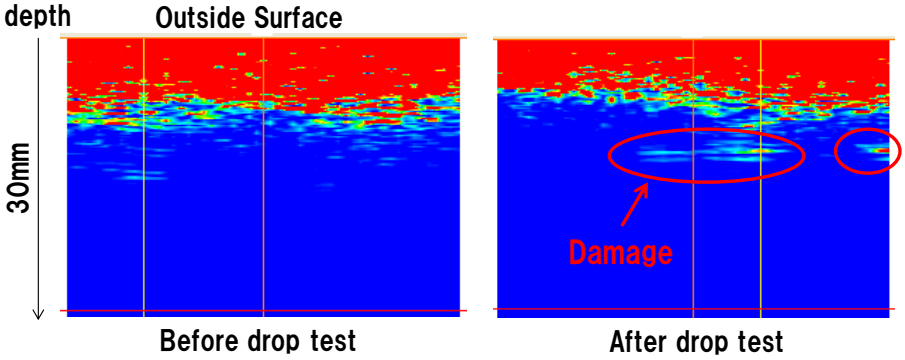

Figure 5. Ultrasonic inspection images (cylindrical part)

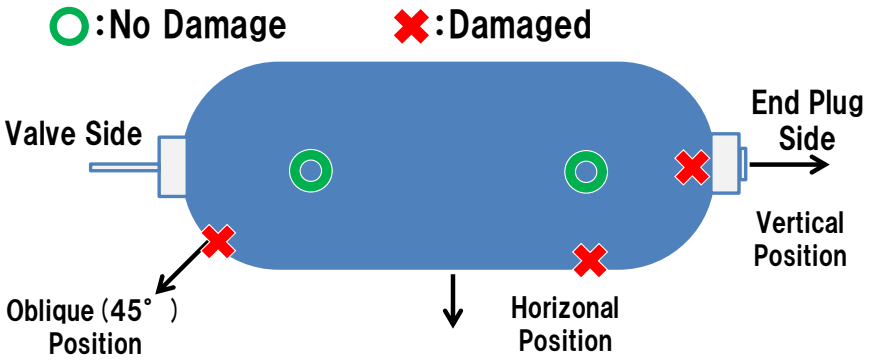

Figure 6. Ultrasonic inspection results

3.2 Investigation of Damage via X-ray CT Imaging

The ultrasonic test results clearly indicate that the drop test damaged the CFRP layer. The damage is considered delamination within the CFRP layer because it is parallel to the container surface [6]. However, a conclusive interpretation cannot be made using only the ultrasonic flaw test results. Therefore, X-ray CT imaging was performed to investigate the damage at the dome part of the containers in more detail. Figure 7 shows the scanning area. The area that extends 50 mm from the CFRP end of the plug side at the dome part of the container was scanned at 0.5 mm intervals in a circular fashion. Furthermore, image analysis software was used to combine the captured images and create a composite 3D image. We investigated the degree of CFRP delamination at the dome part of the container with this composite image. The cross sections of the CT image locations were also compared to the intact condition.

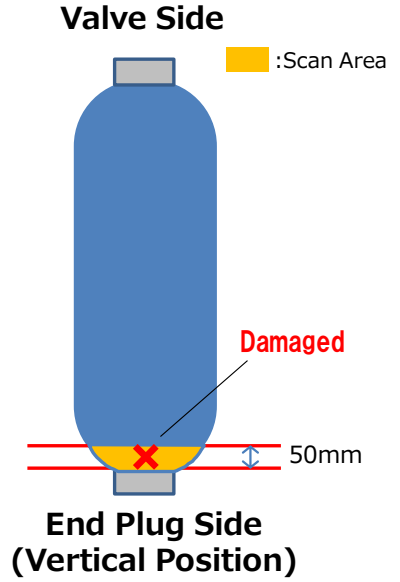

Figure 7. CT scan area

Figure 8 shows a cross section of the plug side at the dome part of the container, both before and after the drop test. The black part in the image is air, the gray part is the CFRP layer, and the white part is the boss (plumbing interface). The CFRP layer contains an air layer after the drop test, it is afraid that an exfoliation is occurred. Furthermore, Figure 9 shows a vertically divided image created by combining the CT images. There were multiple deviations in the middle of the CFRP layer near the boss on the plug side of the container after the drop test. Figure 10 shows a cross-sectional image of the same part of vertically split image created from CT images of dome part. One CFRP layer extends in the direction of the white arrow and forms the dome part by overlapping several layers. These images suggest that this damage is delamination because of the observed exfoliation in the CFRP interlayer portion of the cross-sectional view. The above results indicate that the container damage induced by the drop test is the delamination of the structured CFRP layer. Furthermore, the delamination occurs near the boss on

the plug side by the drop test (vertical drop direction).

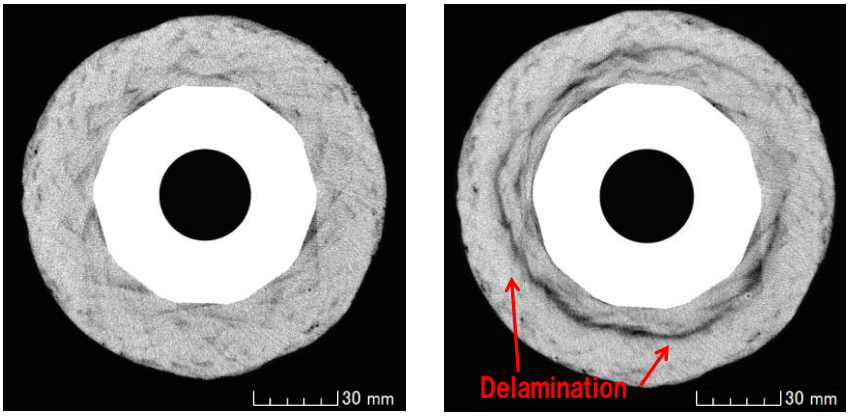

Figure 8. Drop test CT images (horizontal area)

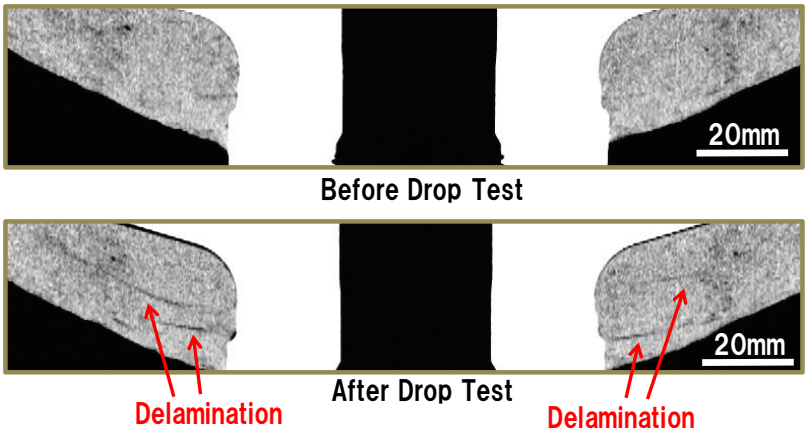

Figure 9. Drop test CT images (vertical area)

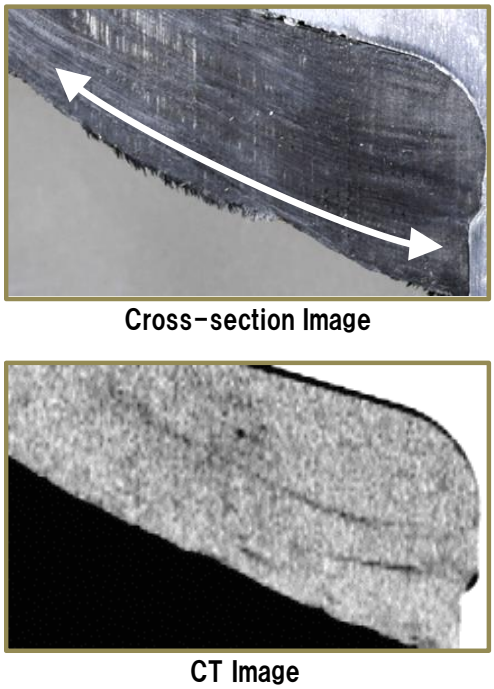

Figure 10. Cross section image and CT image (dome part)

3.3. Investigation of Carbon Fiber Damage at the Damaged Site

The CFRP damage caused by the drop test is considered as a delamination and carbon fiber breakage. The ultrasonic test and X-ray CT imaging indicated that delamination occurred during the drop test, but these investigations cannot observe carbon fiber breakage. Therefore, we conducted a burn-off test to examine the degree of carbon fiber damage within the CFRP layer. A test piece was created from the container after the drop test (Figure 11). This test consisted of cutting a section of the container, including the point of impact from the boss in the dome part, and then creating a test piece from this container section. The test piece was then heated and maintained at approximately 500 °C by using an electric furnace. The CFRP epoxy resin was gasified, and the carbon fiber was extracted. Figure 11 shows the images of the test piece before and after the burn-off test. The test piece was separated into several layers after the burn-off test to investigate the degree of carbon fiber damage within the CFRP layer. Figure 12 shows a representative example of a burn-off test piece. No carbon fiber damage was observed in this test piece. Therefore, the CFRP damage during the vertical drop test was confined to delamination, with no damage to the carbon fibers.

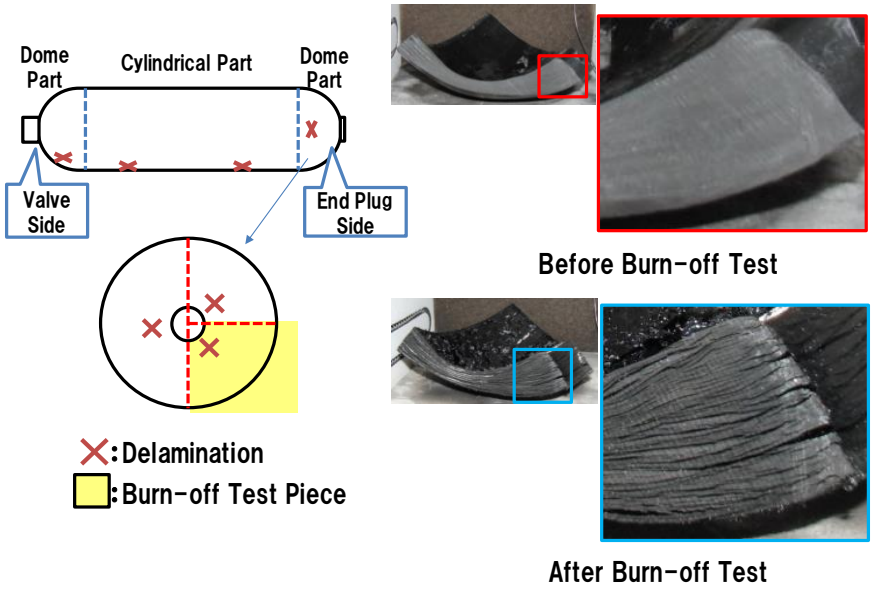

Figure 11. Burn-off test piece

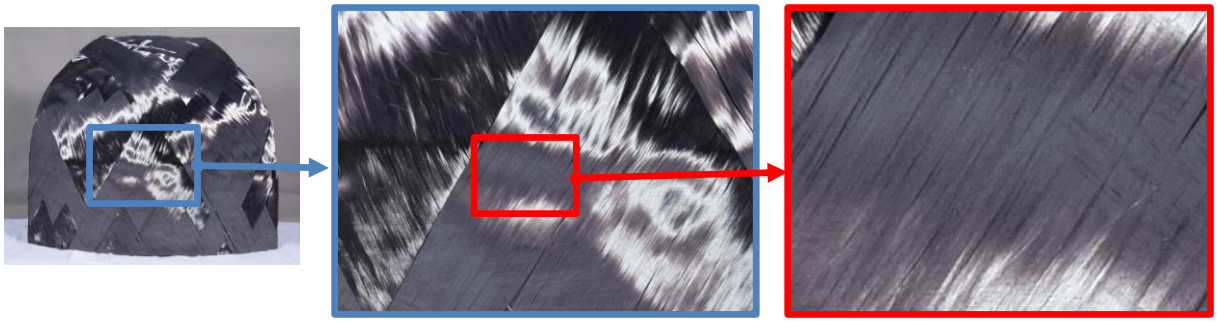

Figure 12. Surface of the test piece after the burn-off test

3.4 Influence of the Pressure Cycling Test on the Drop Test Damage

The ultrasonic flaw detection test and X-ray CT imaging results revealed that the drop test generated delamination in the CFRP layer. However, subsequent pressure cycling test may distort the container, thus possibly propagating delamination. Therefore, X-ray CT imaging was performed on the container after the pressure cycling test to investigate the influence of the pressure cycling on the delamination. The imaging method is the same as that in Section 3.2, with the scan areas up to 50 mm from the plug side at the dome part; the 320 and 720 mm from the plug side, which are the landing sites from the horizontal drop test; and the 520 mm from the plug side, which is the intermediate area (Figure 13).

Figures 14–17 show the images of the plug side at the dome part after a drop test and after a pressure cycling test for comparison. The delamination that existed after the drop test (Figure 14) further developed and became more widespread after the pressure cycling test (Figure 15), with part of the developed interlaminar separation extending to the boss. However, the delamination gap decreased in Figures 16 and 17. This decrease may be due to the applied internal pressure that closed the gap during the pressure cycling test. Figure 18 shows a representative image of the cylindrical part of the container after the pressure cycling test (at a point 320 mm from the plug side). The flaws on the container surface indicated by the green arrows indicate damage from the surface damage test (No. 2 in Figure 1) that was conducted before the pressure cycling test. This test damaged the container surface via two specified types of wire scratches and a pendulum impact, and the green circle shows the cross section of a wire scratch with a depth of 1.25 mm or more. Furthermore, delamination occurred approximately 20 mm away from the container surface of the container to the dome part. The influence of the pressure cycling test on delamination in the cylindrical part of the container is not clarified since no X-ray CT images were acquired after the drop test.

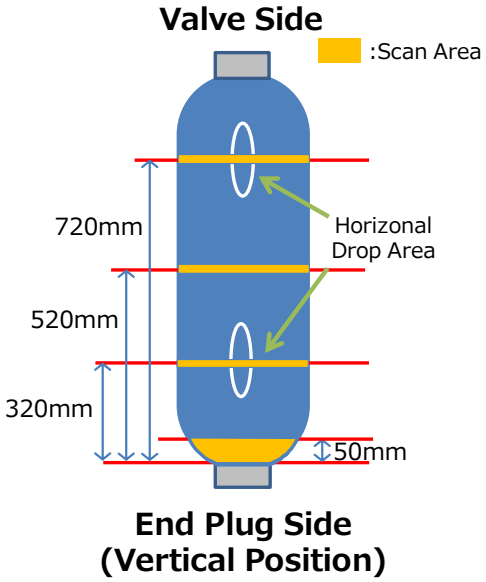

Figure 13. CT scan area (after pressure cycling test)

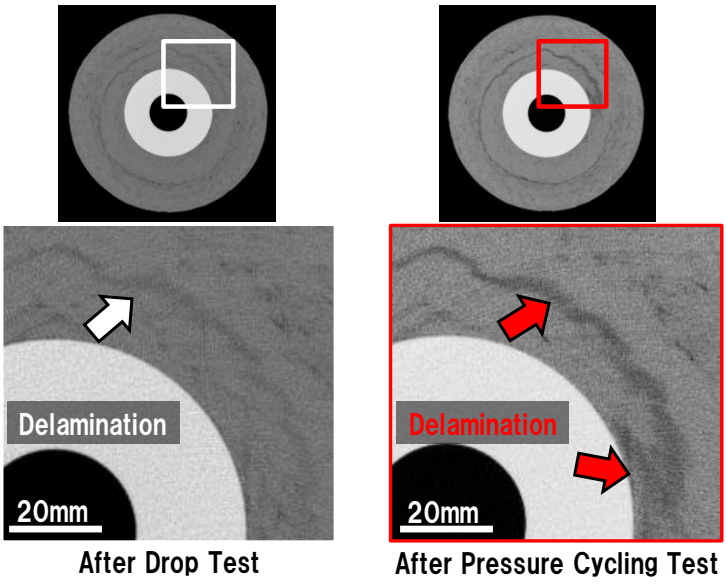

Figure 14. CT images of the horizontal area (delamination growth)

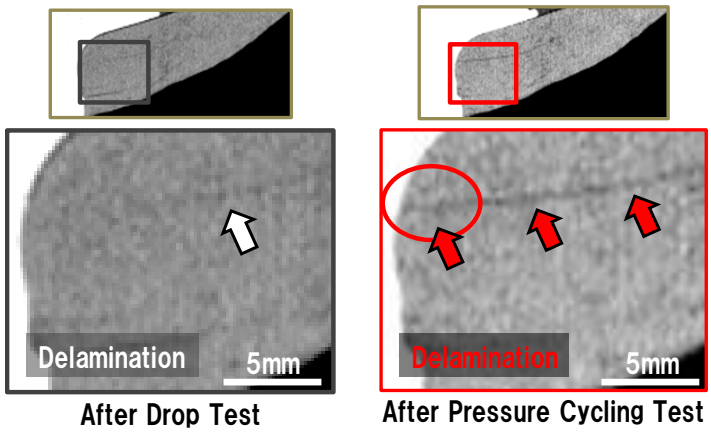

Figure 15. CT images of the vertical area (delamination growth)

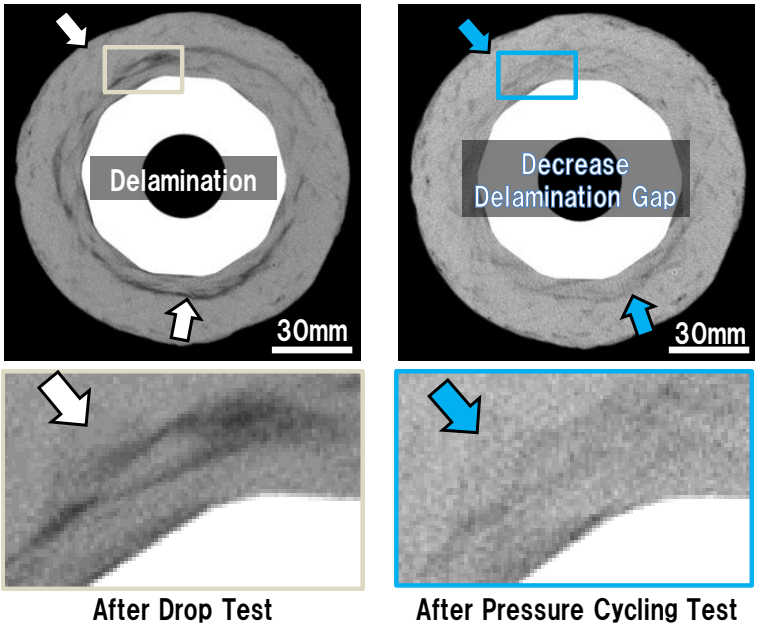

Figure 16. CT images of the horizontal area (decreased delamination gap)

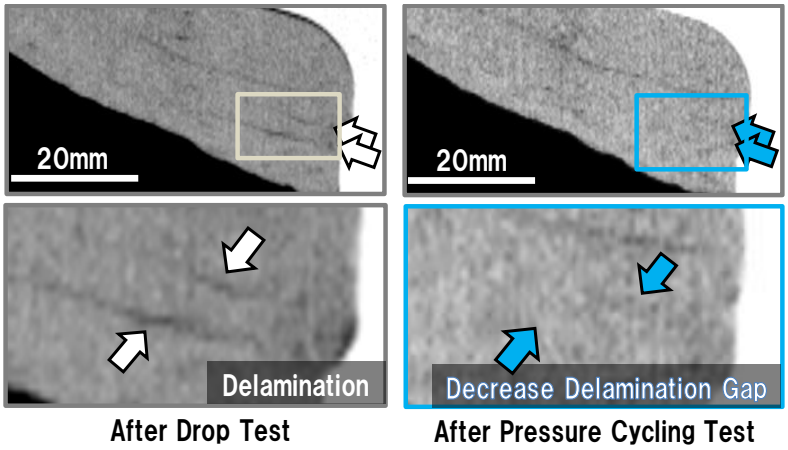

Figure 17. CT images of the vertical area (decreased delamination gap)

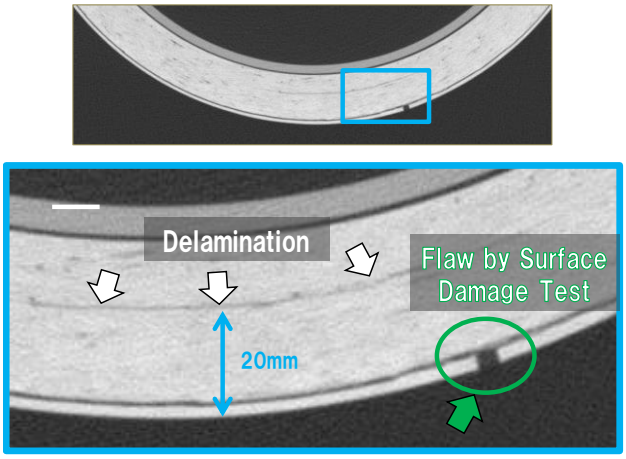

Figure 18. CT images after pressure cycling test (cylindrical part)

4.0 DISCUSSION

The ultrasonic testing and X-ray CT imaging indicated that the drop test caused the delamination of the CFRP layer at the cylindrical and dome parts of the container. Based on that test results, we discuss the influence of the drop damage on burst pressure during the hydraulic sequential tests. The pressure cycling test propagated some of the delamination in the dome part, which was generated via the vertical drop impact. The complex shape of the CFRP layer near the boss indicates that a complex 3D stress will likely be applied to the delamination when the container is distorted during the pressure cycling test. This results in a stress concentration at the delamination tip, which may propagate the delamination in the CFRP layer. Furthermore, some of the developed delamination extended to the boss. This finding suggests that the load sharing of the CFRP layer due to the delamination displacement fluctuates, thus decreasing the burst strength of the dome part. Therefore, delamination propagation during the pressure cycling test may be the primary factor that contributes to the decrease in the burst strength of the dome part. However, the change in the delamination gap in the cylindrical part is unclear due to the lack of CT images before and after the pressure cycling test for comparison. It is necessary to further study the delamination effect of the cylindrical part on the burst pressure. However, it is believed that delamination does not propagate as easily as the dome part because the cylindrical part is in a stable plane stress state that is parallel to the delamination. Furthermore, the carbon fibers in the CFRP layer are partially cut off in the surface damage test (Figure 18). The damage due to the surface damage test becomes the dominant factor in the decreased strength of the cylindrical part because the carbon fiber that is responsible for most of the CFRP strength is divided in the cylindrical part. Therefore, the damage to the cylindrical part via the drop test is expected to have little effect on burst strength.

5.0 CONCLUSIONS

A series of nondestructive evaluations were conducted to investigate the influence of the drop tests on both the container damage and burst pressure during the hydraulic sequential tests, thus yielding the following results:

1. Delamination occurred in the CFRP layer in all drop directions (vertical, horizontal, and oblique [45°] directions) by the drop tests.

2. No carbon fiber damage occurred in the dome part of the container during the vertical drop test, and only delamination was observed in the CFRP layer.

3. The pressure cycling test propagated the delamination of the dome part, and extended some of the delamination to the boss.

The delamination of the dome part of the container generated by the drop test propagates to the boss during the pressure cycling test, with load sharing changes observed in the CFRP layer of the dome part, thus decreasing the burst strength of the dome part. Furthermore, it has been demonstrated that burst pressure variations occurred when the EOL initial rupture point was located at the dome part, thus

suggesting that the strength decreasing of the dome part via the drop test strongly affects the EOL burst pressure. These results indicate that suppressing the drop damage at the dome part is an effective means of preventing the deterioration of the EOL container burst strength. However, in this study, we have only considered the container deterioration mechanism from the observation survey of actual container damage. The strain and stress concentrations of the CFRP layer should be studied via FEM analysis to clarify the detailed mechanism.In addition, in this study, various analytical tests were conducted for only one type of container. Therefore, it is necessary to investigate the drop damage on different types of containers, such as a container conforming the GTR13. In addition, detailed investigations should be conducted on the delamination of the cylindrical part of the container that could not be used in this study.It is necessary to generalize the relation between the degradation mechanism in various containers and the EOL burst pressure by these investigations.

ACKNOWLEDGMENT

This study was conducted as a component of the “Research and Development of Technology for Hydrogen Utilization - Research and Development on Improvement and International Harmonization of compressed hydrogen container regulations for FCV” project commissioned by the New Energy and Industrial Technology Development Organization (NEDO), a national research and development agency of Japan.

REFERENCES

1. Global technical regulation No. 13 - Global technical regulation on hydrogen and fuel cell vehicles, United Nations, 2013.
2. Tomioka, J., Masuda, S., Tamura, H., Tamura, Y., Influences of Hydraulic Sequential Tests on the Burst Strength of Compressed-hydrogen Tanks, *Transactions of Society of Automotive Engineers of Japan*, 49, No. 2, 2018, pp. 296–300.
3. Regulation (EC) No 79 - Type-approval of hydrogen- powered motor vehicles, European Union, 2009.
4. Kamiyama, Y., Komura, I., Furukawa, T., Evaluation of Phased Array UT Applicability using Ultrasonic Visualization Technique, Technical review of JAPEIC, Vol. 9, 2013, pp. 6–10
5. Takagi, H., Murata, I., Fujii, T., Sato, K., et al, High-resolution X-ray CT Image Analysis Technology for the Deformation of the Main Combustion Chamber for Reusable Sounding Rocket Engines, *Journal of JSNDI*, 65, No. 6, 2016, pp. 277–286.
6. Tohgo, K., Material strength analysis, Uchida Roukakuho, Tokyo, 2004, p286–288. (in Japanese)